Advances in Solar Cell Materials and Storage

SOLAR FUELS

Edited by

Nurdan Demirci Sankir
Mehmet Sankir

Scrivener Publishing

WILEY

Solar Fuels

Scrivener Publishing
100 Cummings Center, Suite 541J
Beverly, MA 01915-6106

Advances in Solar Cell Materials and Storage

Series Editor: Nurdan Demirci Sankir and Mehmet Sankir

Scope: Because the use of solar energy as a primary source of energy will exponentially increase for the foreseeable future, this series on *Advances in Solar Cell Materials and Storage* will focus on new and novel solar cell materials and their application for storage. The scope of the series deals with the solution-based manufacturing methods, nanomaterials, organic solar cells, flexible solar cells, batteries and supercapacitors for solar energy storage, and solar cells for space.

Publishers at Scrivener
Martin Scrivener (martin@scrivenerpublishing.com)
Phillip Carmical (pcarmical@scrivenerpublishing.com)

Solar Fuels

Edited by
Nurdan Demirci Sankir
Department of Materials Science and Engineering, TOBB University of Economics and Technology, Ankara, Turkey
and
Mehmet Sankir
Department of Materials Science and Engineering, TOBB University of Economics and Technology, Ankara, Turkey

Scrivener Publishing

WILEY

This edition first published 2023 by John Wiley & Sons, Inc., 111 River Street, Hoboken, NJ 07030, USA and Scrivener Publishing LLC, 100 Cummings Center, Suite 541J, Beverly, MA 01915, USA

For more information about Scrivener publications please visit www.scrivenerpublishing.com.

Wiley Global Headquarters
111 River Street, Hoboken, NJ 07030, USA

For details of our global editorial offices, customer services, and more information about Wiley products visit us at www.wiley.com.

Library of Congress Cataloging-in-Publication Data

ISBN 978-1-119-75057-4

Cover image: Pixabay.Com
Cover design by Russell Richardson

Set in size of 11pt and Minion Pro by Manila Typesetting Company, Makati, Philippines

Printed in the USA

10 9 8 7 6 5 4 3 2 1

Contents

Preface

Among all other energy sources, solar power is the one with the highest capacity and greatest potential. It is humanity's great loss to not be able to use solar energy to produce all the energy we need. This is particularly true since the environmental and sociopolitical problems caused by the use of fossil fuels have negatively affected our future welfare. Therefore, with this as the motivating factor, basic science and engineering studies have been continuing at a rapid pace with the aim of eliminating existing problems to ensure a more efficient and widespread use of solar energy. The biggest disadvantage that solar energy has to face is that it is not accessible at all times of the day and year; in other words, the energy obtained from the sun must be stored.

The energy from photovoltaic systems can be stored in flow batteries or other battery systems, as well as making it storable by converting solar energy to chemical energy, which will make it more cost-effective and versatile compared to the current method. Synthetic chemical fuels obtained by using solar energy are called solar fuels. Hydrogen, methanol, methane, ammonia, carbon monoxide, and some other hydrocarbons and/or oxygenates can be produced from abundant feedstocks such as water, carbon dioxide, and nitrogen via different solar energy-based routes. These routes include solar thermolysis, artificial photosynthesis, and photocatalytic and photoelectrochemical conversion. Therefore, we organized our book to review these routes in informative chapters submitted by distinguished authors. We, as editors, wish to thank the authors for their valuable contributions. This volume covers cutting-edge technologies and materials for efficient solar fuel generation. Additionally, it highlights the research efforts in the literature and adds a valuable component to the area. In addition to the basics, this book also discusses advanced engineering details for both scientists and engineers in academia and industry.

There are four parts and eleven chapters in the book. Part I, Solar Thermochemical and Concentrated Solar Approaches, includes four chapters. Chapter 1 summarizes hydrogen generation via solar thermolysis.

This chapter focuses on the theoretical methods, the state-of-the-art redox-active metal oxides, next-generation perovskite redox-active materials, and materials design directions. Chapter 2 covers recyclable solar transport fuels. In this chapter, all the important aspects of sustainability of solar metal fuels for future long-distance transportation through combustion/reduction cycles are discussed, including direct combustion of solar metal fuels and regeneration of metal fuels through the solar reduction of oxides. Chapter 3 discusses the design and optimization of a standalone plant for hydrogen generation powered by solar energy. Fundamental advances in the copper-chlorine (Cu-Cl) high-performance thermochemical cycle, thermodynamic and economic analyses, and optimization of the system for two objective functions, including the levelized cost of producing hydrogen and solar-to-hydrogen efficiency, are explained in this chapter. Chapter 4 presents a comparative study on solar thermochemical hydrogen production versus solar heat storage using cobalt oxide (Co_3O_4). Among the topics covered are the thermodynamics of direct decomposition of water, a critical analysis of two-step thermochemical water splitting cycles through the redox properties of Co_3O_4, and cyclic thermal energy storage using Co_3O_4.

Part II, Artificial Photosynthesis and Solar Biofuel Production, includes two chapters. Chapter 5 covers the production of biohydrogen from algae. Overall, this chapter intends to summarize the developments in hydrogen production from certain algal species, which is helpful for commercial practice in the near future. Chapter 6 summarizes state-of-the-art applications of photoelectrocatalysis (PEC) in the synthesis of valuable chemicals and solar fuels. This chapter focuses on C-H functionalization in complex organic synthesis, examples of photoelectrochemical-induced C-H activation, C-C functionalization, electrochemically mediated photoredox catalysis, interfacial photoelectrochemistry, and reagent-free cross dehydrogenative coupling.

Part III, Photocatalytic CO_2 Reduction to Fuels, includes two chapters. Chapter 7 focuses on graphene-based catalysts for solar fuels. The preparation of graphene and its composites and the performance of graphene-based catalysts are covered in this chapter. Chapter 8 covers the advances in the design and scale-up of solar fuel systems. Also discussed are strategies for solar photoreactor design, including photocatalytic and electrochemical systems for carbon dioxide reduction, design considerations for scale-up, and future systems and large reactors.

Part IV, Solar-Driven Water Splitting, includes three chapters. Chapter 9 summarizes the advanced materials and systems for solar hydrogen generation. Perovskite ferroelectric nanostructures for photocatalysis and photoelectrocatalysis are also introduced in this chapter. Chapter 10 focuses on photovoltaic-electrolyzer (PVE) systems, consisting of photovoltaic (PV) cells connected by wires with electrolyzers equipped with an anode and a cathode in an electrolyte solution as one of the most promising approaches for solar-driven water splitting. Finally, Chapter 11 offers meaningful guidance to design cost-effective and highly efficient cocatalysts for photocatalytic water splitting. In this context, the basic working principle of cocatalysts and a summary of extensively studied earth-abundant cocatalysts are provided.

In conclusion, we would like to emphasize that this third volume of the *Advances in Solar Cell Materials and Storage* series provides an overall view of the new and highly promising photoactive materials and system designs for solar fuel generation. Therefore, readers from diverse fields, including chemistry, physics, materials science, engineering, and mechanical and chemical engineering, can definitely take advantage of the information presented in this book to better understand the impacts of solar fuels.

Series Editors
Nurdan Demirci Sankir PhD and Mehmet Sankir PhD
Department of Materials Science and Nanotechnology Engineering,
TOBB University of Economics and Technology
February 20, 2023

Part I

SOLAR THERMOCHEMICAL AND CONCENTRATED SOLAR APPROACHES

1

Materials Design Directions for Solar Thermochemical Water Splitting

Robert B. Wexler[1], Ellen B. Stechel[2] and Emily A. Carter[1*]

[1]Department of Mechanical and Aerospace Engineering and the Andlinger Center for Energy and the Environment, Princeton University, Princeton, NJ, United States
[2]ASU LightWorks® and the School of Molecular Sciences, Arizona State University, Tempe, Arizona, United States

Abstract

Solar thermochemical water splitting (STWS) offers a renewable route to hydrogen with the potential to help decarbonize several industries, including transportation, manufacturing, mining, metals processing, and electricity generation, as well as to provide sustainable hydrogen as a chemical feedstock. STWS uses high temperatures from concentrated sunlight or other sustainable means for high-temperature heat to produce hydrogen and oxygen from steam. For example, in its simplest form of a two-step thermochemical cycle, a redox-active metal oxide is heated to ≈1700 to 2000 K, driving off molecular oxygen while producing oxygen vacancies in the material. The reduced metal oxide then cools (ideally with the extracted heat recuperated for reuse) and, in a separate step, comes into contact with steam, which reacts with oxygen vacancies to produce molecular hydrogen while recovering the original state of the metal oxide. Despite its promising use of the entire solar spectrum to split water thermochemically, the estimated cost of hydrogen produced via STWS is ≈4 to 6× the U.S. Department of Energy (DOE) Hydrogen Shot target value of $1/kg.

One contributing approach to bridging this cost gap is the design of new materials with improved thermodynamic properties to enable higher efficiencies. The state-of-the-art (SOA) redox-active metal oxide for STWS is ceria (CeO_2) because of its close to optimal, although too high, oxygen vacancy formation enthalpy and large configurational and electronic entropy of reduction. However, ceria requires high operating temperatures, and its efficiency is insufficient. Therefore, efforts to increase the efficiency of STWS cycles have focused

**Corresponding author*: eac@princeton.edu

Nurdan Demirci Sankir and Mehmet Sankir (eds.) Solar Fuels, (3–64) © 2023 Scrivener Publishing LLC

on further optimizing oxygen vacancy formation enthalpies and augmenting the reduction entropy via substitution or doping and materials discovery schemes. Examples of the latter include the perovskites $BaCe_{0.25}Mn_{0.75}O_3$ and (Ca,Ce)(Ti,Mn)O_3. These efforts and others have revealed intuitive chemical principles for the efficient and systematic design of more effective materials, such as the strong correlation between the enthalpies of crystal bond dissociation and solid-state cation reduction with the enthalpy of oxygen vacancy formation, as well as configurational entropy augmentation via the coexistence of two or more redox-active cation sublattices.

The purpose of this chapter is to prepare the reader with an up-to-date account of STWS redox-active materials, both the SOA and promising newcomers, as well as to provide chemically intuitive strategies for improving their cycle efficiencies through materials design—in conjunction with ongoing efforts in reactor engineering and gas separations—to reach the cost points for commercial viability.

***Keywords*:** Climate change, concentrated solar technologies, hydrogen, solar thermolysis, solar thermochemical cycles, redox-active materials, off-stoichiometric, quantum mechanics simulations

1.1 Introduction

Combatting anthropogenic climate change is one of the critical scientific and engineering challenges of our time. The associated global warming (Figure 1.1a)—predominantly brought about by greenhouse-gas emissions from burning fossil fuels [1–3]—already has led to extreme weather events that threaten the safety and food/water security of life on Earth. Averting the most disastrous effects of climate change calls—at least in part—for clean fuel alternatives to avoid the CO_2 emissions from hard-to-electrify sectors, including heavy-duty vehicles with petroleum-based combustion engines. One encouraging alternative is H_2, which has a higher-energy density per unit mass than liquid hydrocarbons and can be produced using sustainable energy in the form of concentrated solar heat via thermolysis or thermochemical water splitting (Figure 1.1b) [4]. Although not reviewed here, H_2 can also be sustainably produced from water by alternative means, for example, via photoelectrochemical water splitting [5, 6] and both high- [7] and low-temperature [8] electrolysis employing renewable (or nuclear) energy. Concentrated solar technologies (CSTs) also promise to reduce the carbon dioxide footprint of fossil-fuel-derived H_2 from steam-methane reforming, hydrocarbon (fossil or biomass) gasification, solid-oxide electrolysis, and methane cracking.

Two popular solar thermal collector/receiver/reactor designs are the tower with a heliostat field and the parabolic dish (Figure 1.1c) [9]. In the increasingly adopted solar power tower plant architecture, many heliostats focus sunlight on an elevated receiver, achieving a solar concentration ratio (C)—i.e., the factor by which a collector/receiver multiplies the intensity of sunlight impinging upon the Earth's surface—of ≈1000. For parabolic dishes, a polished metal mirror lining concentrates sunlight on a focal point, where redox-active materials could be heated to high temperatures (e.g., 1700–1800 K [10]). While dishes currently are more expensive than towers, they generally lead to a higher C [11] and recently have been used in demonstration CST-based systems [10].

The theoretical maximum efficiency of solar-to-H_2 conversion using CSTs is—under the assumption of ideal optics and a perfectly insulated receiver—the product of the solar collector, receiver, and reactor (Carnot) efficiencies [12, 13]

$$\eta_{solar-to-fuel} = \eta_{collector}\eta_{receiver}\eta_{Carnot} \tag{1.1}$$

$$\eta_{receiver} = 1 - \frac{\sigma T^4}{IC} \tag{1.2}$$

$$\eta_{Carnot} = 1 - \frac{T_{sur}}{T} \tag{1.3}$$

where σ is the Stefan–Boltzmann constant; T the temperature of the receiver; I the intensity of the direct, normal-incident sunlight; and T_{sur} is the temperature of the surroundings (e.g., 298.15 K). Suppose a heliostat field with a solar tower is used instead of a parabolic dish. In that case, $\eta_{collector}$ will be less than one due to factors including the cosine effect (i.e., due to heliostats not pointing directly at the sun and the receiver simultaneously, hence, there is a reduction in the effective reflection area) [14]. One can think of the receiver efficiency ($\eta_{receiver}$) as the fraction of absorbed sunlight that is not reradiated by the blackbody-like receiver. Increasing C can increase the T range over which $\eta_{receiver}$ is close to 100%. For example, if parabolic dishes—with C reaching 10000—can be made economical, then a nearly perfect receiver can be achieved at ≈2000 K (Figure 1.1d,

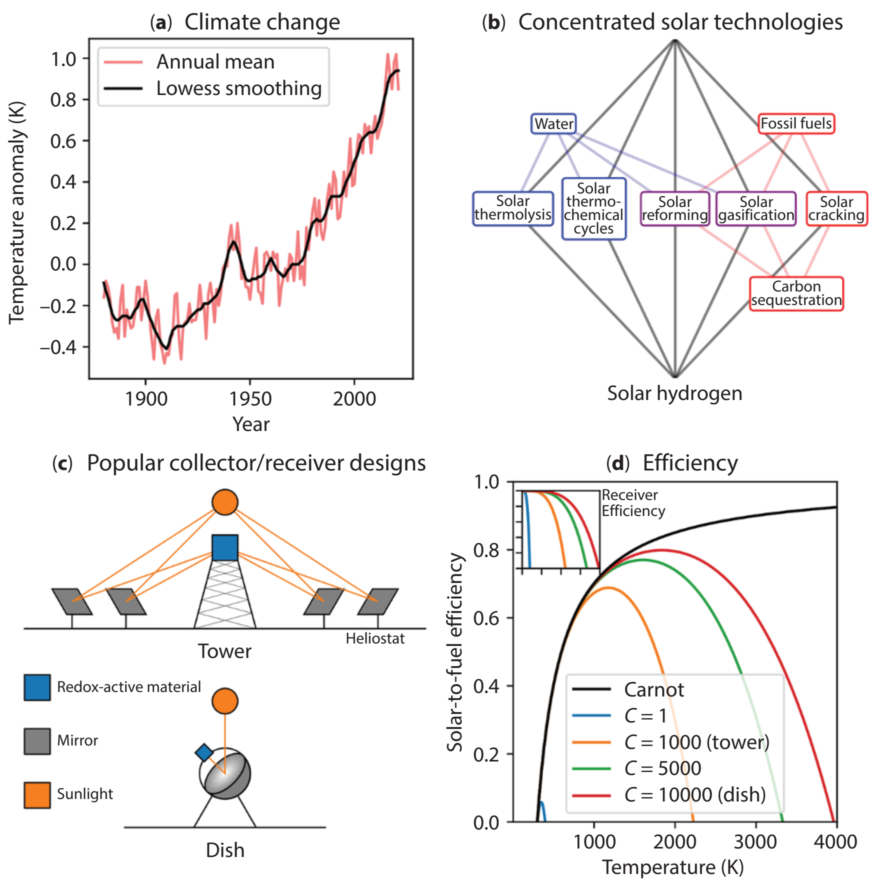

Figure 1.1 Concentrated solar hydrogen for combatting climate change. (a) Increase in global temperature since 1880. (b) Routes to solar hydrogen via concentrated solar technologies. (c) Popular collector/receiver designs for concentrated solar heat technologies. (d) Ideal solar-to-fuel efficiency ($\eta_{solar\text{-}to\text{-}fuel}$ in Equation (1.1)) and (d, inset) receiver efficiency ($\eta_{receiver}$ in Equation (1.2)—with the same ticks and tick labels as the larger panel). Note that towers can have $C > 1000$ and developing dishes with $C = 10{,}000$ is quite challenging. That said, we chose these values to indicate the effect of order-of-magnitude changes in C on the theoretical solar-to-fuel efficiency.

inset). While $\eta_{receiver}$ dominates $\eta_{solar\text{-}to\text{-}fuel}$ in the high-temperature limit, the efficiency of a Carnot engine (η_{Carnot}) governs the low-temperature regime, which decreases to zero as T approaches T_{sur} from above. Upon multiplying these three efficiencies, it becomes clear that—for a given C—there is an ideal temperature at which $\eta_{solar\text{-}to\text{-}fuel}$ is maximized (Figure 1.1d). As an example, consider a dish that provides C = 5000. If the receiver is heated to 1800 K, one can use ≤76% of the concentrated sunlight energy for solar-to-H_2 conversion. Here, the "less than" indicates that other loss mechanisms and engineering constraints typically produce efficiencies << 76%.

1.1.1 Hydrogen via Solar Thermolysis

Having introduced CSTs and their efficiencies for a general solar-to-H_2 process, we now consider the earliest and perhaps simplest approach to CST-based hydrogen production via solar thermolysis or *direct* solar water splitting [15]. In solar thermolysis, H_2O(g) is heated to $T \geq 2500$ K, above which it can undergo the following high-temperature reactions (Figure 1.2a) [16]:

Blue line $$H_2O(g) \rightleftharpoons H_2(g) + \frac{1}{2}O_2(g) \tag{1.4}$$

Orange line $$H_2(g) \rightleftharpoons 2H(g) \tag{1.5}$$

Green line $$\frac{1}{2}O_2(g) \rightleftharpoons O(g) \tag{1.6}$$

Red line $$H_2O(g) \rightleftharpoons H(g) + OH(g) \tag{1.7}$$

At $T < 2000$ K and $p = 1$ bar, none of these reactions occur with appreciable yields, leaving H_2O(g) intact (Figure 1.2b). As T reaches 2500 K, ≈4% of H_2O(g) molecules split into H_2(g) and O_2(g) (Equation 1.4). For $T > 2500$ K, however, side reactions—such as the atomization of H_2(g) (Equation 1.5) and O_2(g) [Equation (1.6)], and the dissociation of H_2O(g) into H(g) and OH(g) (Equation 1.7)—compete with the desired water-splitting reaction, leading to a maximum H_2(g) mole fraction of ≈0.19 at 3400 K. In addition to its upper limit for H_2 generation, solar thermolysis is impractical [17] because it produces an explosive mixture of H_2(g) and O_2(g) that requires careful separation and rapid quenching to avoid recombination, which reduces efficiency. Furthermore, the T needed to produce H_2(g) and not

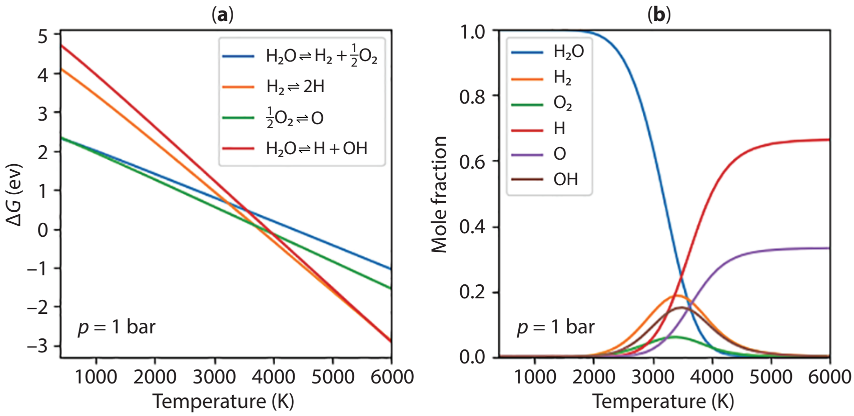

Figure 1.2 Thermodynamics of hydrogen production via solar thermolysis. (a) Gibbs free energy change (ΔG) of high-temperature reactions at p = 1 bar. (b) Equilibrium mole fractions at p = 1 bar (see Appendix A. Equilibrium Composition for Solar Thermolysis).

H(g) or OH(g)—i.e., ≈2500 K—leads to the thermal failure of the ceramics used for H_2(g) and O_2(g) separation, thus motivating—in the absence of solutions for these issues—another route to solar H_2, namely solar thermochemical water splitting (STWS) [18–26].

1.1.2 Hydrogen via Solar Thermochemical Cycles

To split water at lower temperatures and preclude the formation of undesired gas-phase molecules, one can employ thermochemical cycles, the simplest of which—and the primary subject of this book chapter—is a two-step cycle [27–34] (Figure 1.3a) with redox-active, metal-oxide materials (Figure 1.3b). In such a cycle, a metal oxide (MO_x, where x is the number of moles of O per cation) first is heated, using CSTs, to temperatures typically exceeding 1500 K and most often close to 1800 K, at which point it is reduced to a more O-poor stoichiometry ($MO_{x-\delta}$), i.e.,

$$\frac{1}{\delta}MO_x(s) \rightleftharpoons \frac{1}{\delta}MO_{x-\delta} + \frac{1}{2}O_2(g) \tag{1.8}$$

where δ is the off-stoichiometry; note that we have purposefully omitted the phase of the reduced metal oxide for reasons to be explained momentarily. Generally speaking, one would reduce at the highest temperatures within engineering and economic constraints to ensure maximal reduction (as increasing the temperature makes Δ*G* more negative and therefore increases δ) and fast kinetics. In the second step, the reduced metal oxide cools to a temperature where reoxidation is possible when exposed to H_2O(g), which leads to water splitting and regeneration of the original metal oxide, i.e.,

$$\frac{1}{\delta}MO_{x-\delta}+H_2O(g)\rightleftharpoons\frac{1}{\delta}MO_x(s)+H_2(g) \tag{1.9}$$

Generally, $MO_{x-\delta}$ will not reoxidize to the fully stoichiometric form MO_x but will cycle between two forms of the metal-oxide stoichiometry—both partially reduced—where the difference between the two off-stoichiometries is one of the performance metrics. The reoxidation is further limited if there is a small amount of hydrogen in the gas stream, which might be expected if one separates, in the gas phase, the hydrogen from the reoxidation product stream and recycles any unconverted steam.

Unlike thermal reduction (Equation 1.8), whose ideal operating temperature is bounded only from above by the thermal stability of the material and durability of the reactor, one would perform water splitting (Equation 1.9) at temperatures high enough for fast kinetics but low enough for a good Δ*G* of reoxidation. This compromise often requires water splitting to be done around 1000 K or higher. Another consideration is recuperation of heat between the high temperature and low temperature steps. The larger the temperature difference, the greater the engineering challenge to limit the losses.

Until now, we have neither specified the phase of $MO_{x-\delta}$ nor the extent of reduction δ. Two-step metal-oxide thermochemical cycles are based on either volatile or non-volatile metal oxides. Volatile refers to a metal oxide for which a solid-to-gas phase transition accompanies thermal reduction. One of the most widely studied volatile cycles is ZnO(s)/Zn(g) [35–37]:

$$ZnO(s)\rightleftharpoons Zn(g)+\frac{1}{2}O_2(g) \tag{1.10}$$

$$Zn(s)+H_2O(g)\rightleftharpoons ZnO(s)+H_2(g) \tag{1.11}$$

In the thermal reduction step [Equation (1.10)], which one must carry out at temperatures above 2000 K, ZnO(s) volatilizes to Zn(g) and O_2(g). While the ZnO(s)/Zn(g) cycle offers favorable efficiencies even in the absence of heat recovery (energy conversion efficiency ≈ 45% and maximum exergy efficiency ≈ 29%), its issues are similar to those faced in solar thermolysis in that the high temperatures required for significant reduction put a considerable thermal strain on the receiver/reactor [17, 38]. After thermal reduction, one generally quenches quickly to avoid the back reaction before separating Zn(s) from O_2(g). Alternatively, electrothermal gas-phase separation has been considered [39, 40]. Water splitting [Equation (1.11)], on the other hand, typically takes place at $T \leq 900$ K, revealing another difficulty for ZnO(s)/Zn(g): the need for a giant temperature swing (≥1100 K). Other redox couples for volatile, two-step STWS have been considered, such as post-transition-metal oxides in the SnO_2(s)/SnO(g) cycle [41–43]; however, those with greater attention currently are solid phase, a.k.a. non-volatile, redox-active materials.

Within non-volatile, redox-active metal oxides, the two main categories are stoichiometric (line compounds) and off-stoichiometric. First, we consider stoichiometric metal oxides, where stoichiometric refers to materials for which reduction and reoxidation produce pure, solid-phase, metal-containing compounds obeying full stoichiometry constraints on composition. One can further subdivide stoichiometric metal oxides into single-component and multi-component compositions. Examples best illustrate the difference between these two types of stoichiometric oxides. The prototypical single-component materials are metal-doped ferrites [44–54], whose thermal reduction and water splitting reactions are

$$(M_xFe_{1-x})_3O_4(s) \rightleftharpoons 3xMO(s) + 3(1-x)FeO(s) + \frac{1}{2}O_2(g) \quad (1.12)$$

$$3xMO(s) + 3(1-x)FeO(s) + H_2O(g) \rightleftharpoons (M_xFe_{1-x})_3O_4(s) + H_2(g) \quad (1.13)$$

where the metal (M) dopant or substituent can be Fe (in which case Fe is not a dopant and the phase is magnetite) [55–59], Zn [60], Ni [60, 61], Co [60, 62] (as well as a complete replacement of Fe with Co [63]), Mn [61], and others. Ferrites with other metals substituted in the spinel or inverse spinel structure can be tuned to provide nearly optimal reduction Gibbs free energetics and reduction temperatures lower than 2000 K [64, 65]. However, both their reduction and water-splitting kinetics are slow because O^{2-} is close-packed in both oxide structures, Fe_3O_4 and FeO(s). Therefore, it does not react beyond the surface [66]. Additionally, powdered Fe oxides sinter, rendering them uncyclable [56, 62, 67, 68]. To enhance cyclability, one can use yttria-stabilized zirconia as an inert support that incorporates active Fe ions into its crystal lattice, forming a solid solution, thus alleviating the sintering or melting of iron oxides at the working temperatures of 1200 to 1700 K [55, 69]. Note that, for ferrite cycles, a single metal oxide reduces and reoxidizes, hence the terminology "single component."

Alternatively, multi-component cycles involve the redox of more than one metal oxide component. An excellent example of this case is the cycle based on the mineral hercynite $FeAl_2O_4(s)$ [70–77]:

$$CoFe_2O_4(s)+3Al_2O_3(s) \rightleftharpoons CoAl_2O_4(s)+2FeAl_2O_4(s)+\frac{1}{2}O_2(g) \tag{1.14}$$

$$CoAl_2O_4(s) + 2FeAl_2O_4(s) + H_2O(g) \rightleftharpoons CoFe_2O_4(s) + 3Al_2O_3(s) + H_2(g) \tag{1.15}$$

During thermal reduction, $CoFe_2O_4(s)$—a metal-substituted ferrite—reacts with three moles of $Al_2O_3(s)$, producing $CoAl_2O_4(s)$—a pigment known as cobalt blue—along with two moles of hercynite and a half mole of $O_2(g)$. These intermediate products then split water at lower temperatures, restoring the original solids in their starting stoichiometric coefficients and generating $H_2(g)$. Both steps have two metal-oxide components in the reactants and products, so the hercynite cycle is multi-component. However, like the ferrites, this cycle suffers from poor kinetics, which is unsurprising considering one of the components is cobalt ferrite $CoFe_2O_4(s)$. Other studied multicomponent cycles include—but are not limited to—those based on the metal sulfate/oxide [e.g., $MnSO_4(s)/MnO(s)$ [78]] and metal dioxide/pyrochlore [i.e., $CeO_2(s)+MO_2(s)/Ce_2M_2O_7(s)$ where M can be, e.g., Ti [79], Si [79], or Sn [80]] redox couples. Ultimately, kinetic limitations are a hallmark of stoichiometric materials because their STWS cycles require the nucleation and growth of bulk phases. A promising path to promote faster kinetics is to use off-stoichiometric metal oxides, which tend to be mixed ionic-electronic conductors (MIECs) that form and fill oxygen vacancies (V_Os) during thermal reduction and water splitting, respectively, instead of undergoing major bulk structural phase transitions. As off-stoichiometric metal oxides, particularly MIECs because of their superior ion diffusion kinetics, currently are the subject of intense research for STWS applications and are the redox-active materials of choice for pilot plants, we focus on them here. Below we emphasize developing intuition that explains observed physicochemical phenomena, in order to determine materials design criteria that can lead to tailoring materials for more optimal thermochemical cycles.

Before we dive into the details of off-stoichiometric metal oxides for STWS, we would be remiss if we did not mention the utility of multi-step cycles. We will first describe the Cu-Cl [81] cycle (Figure 1.3c). In the hydrolysis step, Cu(II)Cl_2(s) is heated to ≈673 K in the presence of H_2O(g),

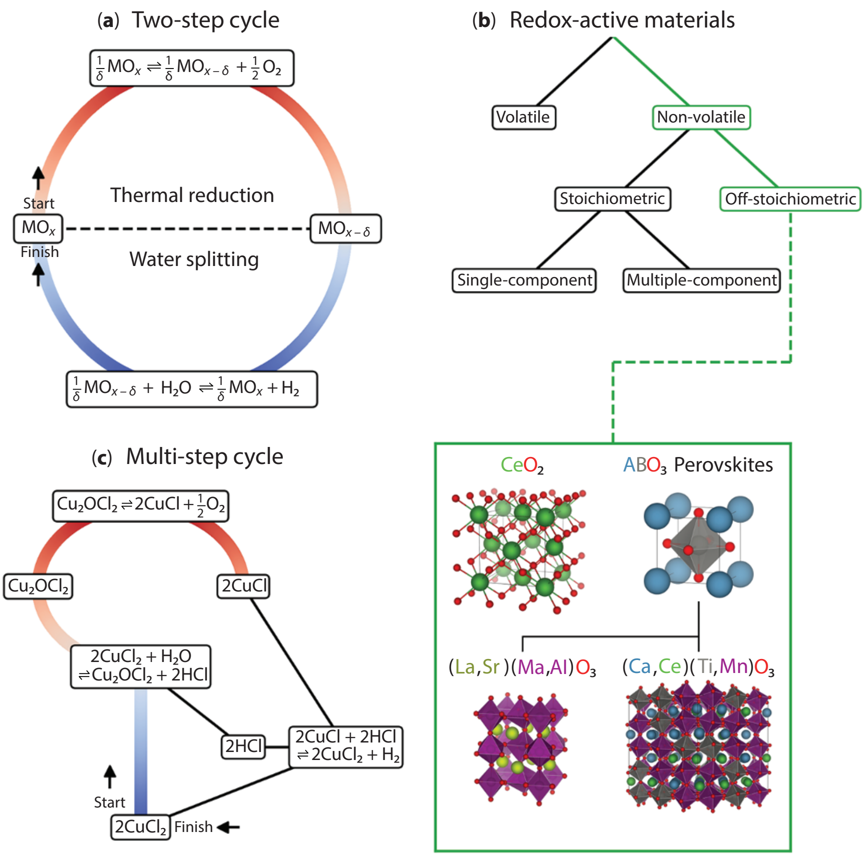

Figure 1.3 Hydrogen production via solar thermochemical cycles. (a) Schematic of a two-step cycle for a metal oxide (MO_x) that becomes off-stoichiometric ($MO_{x-\delta}$, where δ is the off-stoichiometry) upon thermal reduction (where the color of the circle denotes relative temperature). (b) Types of redox-active materials typically employed for two-step STWS, where our focus is on nonvolatile materials that become off-stoichiometric upon thermal reduction, such as CeO_2 and ABO_3 perovskites and their alloys. (c) Schematic of a multistep cycle, specifically, here, the copper chloride hybrid cycle, which involves hydrolysis (blue), thermal reduction (red), and electrolysis (black) steps at different temperatures.